A Novel Method of Moments for Numerical Analysis of Antennas Over 2-D Infinite Periodic Arrays of Scatterers

Keisuke Konno, *Member, IEEE*, Nozomi Haga, *Member, IEEE*, Jerdvisanop Chakarothai, *Senior Member, IEEE*, Qiang Chen, *Senior Member, IEEE*, Narihiro Nakamoto, *Member, IEEE*, and Toru Takahashi, *Senior Member, IEEE*

***Abstract*— In this article, a novel method of moments (MoM) for numerical analysis of antennas over a 2-D infinite periodic array of scatterers is proposed. The proposed MoM models the 2-D infinite periodic array of scatterers as a reflecting plane, i.e., electromagnetic response of the 2-D infinite periodic array of scatterers is formulated via their reflection coefficient. In a similar manner to a layered media Green's function, self/mutual coupling between source and observation points over the 2-D infinite periodic array of scatterers is formulated as a superposition of direct wave component and TE/TM reflection wave components. Numerical simulation is performed, and performance of the proposed MoM is demonstrated. The proposed MoM has a couple of advantages. The first and second ones are mesh-free/numerical modelings of the 2-D infinite periodic array of scatterers via their reflection coefficient. The mesh-free modeling contributes to small computational cost whereas the numerical modeling enables to deal with the 2-D infinite periodic array of arbitrary-shaped scatterers. The third one is ease of combination with existent numerical analysis tool of the 2-D infinite periodic array of scatterers.**

***Index Terms*— Method of moments (MoM), periodic Green's function.**

I. Introduction

AN INFINITE periodic array of scatterers has been widely used for modeling frequency selective surfaces (FSSs), metamaterials, and unitcells of reflectarrays [1], [2], [3]. Numerical analysis of the infinite periodic array of scatterers has been one of the classic problems and so-called periodic boundary condition is well known as an efficient approach for their modeling during numerical analysis [4]. According to the periodic boundary condition, the infinite periodic array of scatterers is reduced to an unitcell. As a result, scattering performance of the infinite periodic array of scatterers can be obtained efficiently. For example, method of moments (MoM) with periodic Green's function is a powerful technique for numerical analysis of the infinite periodic array of scatterers under the periodic boundary condition [5], [6], [7]. Owing to recent advancement of commercial simulator software, numerical analysis of the infinite periodic array of scatterers under the periodic boundary condition can be performed easily.

On the other hand, antennas over a periodic array of scatterers have been developed so far. For example, the antennas over artificial magnetic conductor (AMC) have been proposed for suppressing mutual coupling between antennas or designing low-profile antennas [8]. A photonic bandgap (PBG) structure has been introduced as a ground plane of the reflectarrays for enhancing their gain [9]. Although numerical analysis of the infinite periodic array of the scatterers can be performed efficiently under the periodic boundary condition, numerical analysis of the antennas over the periodic array of the scatterers cannot be performed efficiently. For example, one of the straightforward approaches is full-wave analysis of the antennas over a finite periodic array of the scatterers. Effect of the finite periodic array of the scatterers on the performance of the antennas can be obtained accurately using this straightforward approach but this approach is often computationally too expensive because the periodic array of the scatterers is modeled as a finite and large array. Of course, so-called fast MoM such as a characteristic basis function method (CBFM) [10], [11], [12] or a conjugate gradient method combined with discreate/fast Fourier transform [13], [14], [15] is helpful for reducing the computational cost, but the large computational cost is still inevitable as the number of the scatterers increases. Another approach is to enforce the periodic boundary condition for modeling the antennas over the periodic array of the scatterers. This approach is computationally efficient but poor accuracy is expected because the antennas themselves are not always

Manuscript received 23 March 2023; revised 29 June 2023; accepted 31 July 2023. Date of publication 11 August 2023; date of current version 9 February 2024. This work was supported by the JSPS KAKENHI under Grant 22K04061. *(Corresponding author: Keisuke Konno.)*

Keisuke Konno and Qiang Chen are with the Department of Communications Engineering, Graduate School of Engineering, Tohoku University, Sendai 980-8579, Japan (e-mail: keisuke.konno.b5@tohoku.ac.jp).

Nozomi Haga is with the Department of Electrical and Electronic Information Engineering, Toyohashi University of Technology, Toyohashi 441-8580, Japan (e-mail: haga.nozomi.ok@tut.jp).

Jerdvisanop Chakarothai is with the National Institute of Information and Communications Technology, Koganei 184-8795, Japan (e-mail: jerd@nict.go.jp).

Narihiro Nakamoto and Toru Takahashi are with Mitsubishi Electric Corporation, Kamakura 247-8501, Japan (e-mail: nakamoto.narihiro@ap.mitsubishielectric.co.jp).

Color versions of one or more figures in this article are available at https://doi.org/10.1109/TAP.2023.3303025.

Digital Object Identifier 10.1109/TAP.2023.3303025

the periodic arrays. As mentioned here, an efficient numerical analysis method of the antennas over the periodic array of the scatterers is expected to be developed.

Extensive efforts have been dedicated to developing the efficient numerical analysis method of the antennas over the periodic array of the scatterers. Array scanning method (ASM) is an approach to obtain a field radiated from a single source point over the periodic array of scatterers [16], [17], [18], [19], [20], [21], [22], and [23]. The radiated field from a single line or dipole source is reconstructed from the radiated field of an array of the line or dipole sources whose periodicity is the same as that of the scatterers. Although the ASM is computationally efficient, performance of the ASM has been demonstrated only for ideal sources over the periodic array of the scatterers. It has not been demonstrated that the ASM is applicable for numerical analysis of practical antennas over the periodic array of arbitrary-shaped scatterers. A surface impedance model has been introduced to a dyadic Green's function for modeling the periodic array of the scatterers [24], [25]. Although the surface impedance model is applicable to the periodic array of the practical scatterers such as microstrip patches, its applicability is limited because a closed form expression of the surface impedance is only available for a specific periodic array of scatterers, such as an array of patches over a substrate [26]. Moreover, numerical results of the MoM using the dyadic Green's function with the surface impedance model are absent for the works. The surface impedance model has been combined with finite difference time domain (FDTD) method and applied to numerical analysis of a dipole antenna over a metasurface composed of a rectangular patch on a dielectric slab [27]. It has been reported that accuracy of input impedance of the dipole antenna is insufficient whereas its radiation pattern shows good agreement with that of the dipole antenna over the finite periodic array. To the best of our knowledge, an efficient numerical analysis method for arbitrary-shaped antennas over the 2-D infinite periodic array of arbitrary-shaped scatterers has not been proposed so far.

In this article, a novel MoM for numerical analysis of antennas over a 2-D infinite periodic array of scatterers is proposed. The proposed MoM deals with the 2-D infinite periodic array of scatterers as a reflecting plane and their electromagnetic response is modeled via reflection coefficients. In a similar manner to a layered media Green's function, self/mutual coupling between source and observation points over the 2-D infinite periodic array of scatterers is formulated as a superposition of a direct wave component and TE/TM reflection wave components. The direct wave component is expressed using the free-space Green's function whereas the TE/TM reflection wave components are expressed using the numerically obtained reflection coefficients combined with a plane wave expansion. Owing to the formulation of the electromagnetic response of the 2-D infinite periodic array of scatterers via reflection coefficients, the proposed MoM is mesh-free for the 2-D infinite periodic array of scatterers. Moreover, the proposed MoM is applicable to numerical analysis of arbitrary-shaped antennas over the 2-D infinite periodic array of arbitrary-shaped scatterers.

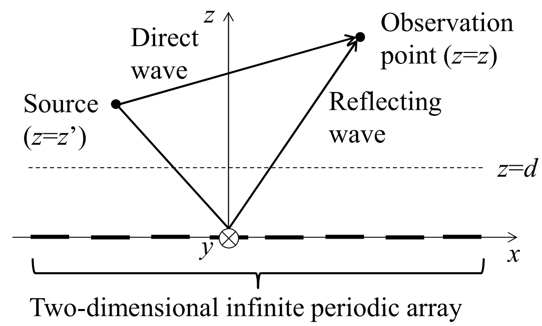

Fig. 1. Source and observation points over 2-D infinite periodic array of scatterers.

This article is organized as follows. Formulation of the proposed MoM is described in Section II. Numerical simulation is performed, and performance of the proposed MoM is demonstrated in Section III. Finally, this article is concluded in Section IV.

II. Formulation

Fig. 1 shows source and observation points over a 2-D infinite periodic array of scatterers. Here, self/mutual coupling between the source and the observation points over the 2-D infinite periodic array of scatterers is formulated under following assumptions.

1) The reflection coefficients of the 2-D infinite periodic array of scatterers are numerically obtained at $z = d$, where d is the height of a reference plane of the reflection coefficients.
2) The source and the observation points are above the reference plane of their reflection coefficients, i.e., $z' > d$ and $z > d$.
3) Effect of reflecting wave corresponding to evanescent wave on self/mutual coupling is neglected because of simplicity. This assumption is justified when the source and observation points are away from the 2-D infinite periodic array of scatterers. Mathematically, this assumption can be described as $k_z^2 = k_0^2 - k_x^2 - k_y^2 \geq 0$. Here, k_0 is wavenumber in free space. $k_x = k_0 \sin\theta \cos\phi$, $k_y = k_0 \sin\theta \sin\phi$, and $k_z = k_0 \cos\theta$ are wave numbers in free space corresponding to x-, y-, and z-directions, respectively.

A. Propagation Factor

In the same manner, as derivation of the layered media Green's function, so-called propagation factor between the source and the observation points is described in a spectral domain as follows [28]:

$$F = e^{-jk_z|z-z'|} + Be^{-jk_{z}z} \tag{1}$$

where $e^{-jk_z|z-z'|}$ corresponds to direct wave from the source point to the observation point whereas $e^{-jk_{z}z}$ corresponds to reflection wave from the 2-D infinite periodic array of scatterers. B is unknown coefficient of the reflection wave. Since the reflection wave at $z = d$ results from reflection of the direct wave by the 2-D infinite periodic array of scatterers, unknown coefficient B is expressed as follows:

$$\begin{aligned} Be^{-jk_z d} &= \Gamma_{z=0}(\theta,\phi)e^{-jk_z|d-z'|} \\ B &= \Gamma_{z=0}(\theta,\phi)e^{-jk_z\left(z'-2d\right)} \quad \left(\because z' > d\right) \\ &= \Gamma_{z=d}(\theta,\phi)e^{-jk'_z z} \end{aligned} \tag{2}$$

where $\Gamma_{z=d}(\theta,\phi) = \Gamma_{z=0}(\theta,\phi)e^{j2\ k_z d}$ is the reflection coefficient of the 2-D infinite periodic array of scatterers at $z = d$. Finally, (2) is substituted into (1), the propagation factor is obtained as follows:

$$F = e^{-jk_z|z-z'|} + \Gamma_{z=d}(\theta,\phi)e^{-jk_z\left(z'+z\right)}. \tag{3}$$

According to (3), the propagation factor corresponding to TE and TM reflection waves can be described as follows:

$$F^{\mathrm{TE/TM}} = \Gamma_{z=d}^{\mathrm{TE/TM}}(\theta,\phi)e^{-jk_z\left(z'+z\right)}. \tag{4}$$

It should be noted that $\Gamma_{z=d}^{\mathrm{TE}}(\theta,\phi)$ in (4) is the reflection coefficient of the electric field whereas the $\Gamma_{z=d}^{\mathrm{TM}}(\theta,\phi)$ is the reflection coefficient of the magnetic field [28].

B. Reduced Forms of Dyadic Green's Functions

Once electromagnetic response from the 2-D infinite periodic array of scatterers is described via their reflection coefficient, the 2-D infinite periodic array of scatterers can be modeled as a reflecting plane whose reflection coefficient is known. As a result, self/mutual coupling between the source and observation points over the 2-D infinite periodic array of scatterers can be described in the same manner as the layered media Green's function as follows [28], [29], [30]:

$$\overline{\overline{\mathbf{G}}}(\mathbf{r},\mathbf{r}') \approx \overline{\overline{\mathbf{G}}}^{\mathrm{D}}(\mathbf{r},\mathbf{r}') + \overline{\overline{\mathbf{G}}}^{\mathrm{TE}}(\mathbf{r},\mathbf{r}') + \frac{1}{k_0^2}\overline{\overline{\mathbf{G}}}^{\mathrm{TM}}(\mathbf{r},\mathbf{r}')$$

$$\begin{aligned} \overline{\overline{\mathbf{G}}}^{\mathrm{D}}(\mathbf{r},\mathbf{r}') &= \left(\overline{\overline{\mathbf{I}}} + \frac{\nabla\nabla}{k_0^2}\right)\frac{e^{-jk_0|\mathbf{r}-\mathbf{r}'|}}{4\pi|\mathbf{r}-\mathbf{r}'|} \\ &\approx \left(\overline{\overline{\mathbf{I}}} + \frac{\nabla\nabla}{k_0^2}\right)\left(\frac{-jk_0}{8\pi^2}\right) \\ &\quad \int_0^{2\pi}\int_0^{\frac{\pi}{2}} e^{-j\mathbf{k}\cdot(\mathbf{r}-\mathbf{r}')}\sin\theta d\theta d\phi \end{aligned} \tag{5}$$

$$\overline{\overline{\mathbf{G}}}^{\mathrm{TE}}(\mathbf{r},\mathbf{r}') \approx \frac{-jk_0\hat{\boldsymbol{\phi}}\hat{\boldsymbol{\phi}}}{8\pi^2}\int_0^{2\pi}\int_0^{\frac{\pi}{2}} e^{-j\mathbf{k}_{xy}\cdot\left(\boldsymbol{\rho}_{xy}-\boldsymbol{\rho}'_{xy}\right)} F^{\mathrm{TE}}\sin\theta d\theta d\phi \tag{6}$$

$$\overline{\overline{\mathbf{G}}}^{\mathrm{TM}}(\mathbf{r},\mathbf{r}') \approx \frac{-jk_0^3\hat{\boldsymbol{\theta}}\hat{\boldsymbol{\theta}}}{8\pi^2}\int_0^{2\pi}\int_0^{\frac{\pi}{2}} e^{-j\mathbf{k}_{xy}\cdot\left(\boldsymbol{\rho}_{xy}-\boldsymbol{\rho}'_{xy}\right)} F^{\mathrm{TM}}\sin\theta d\theta d\phi. \tag{7}$$

Here, $\mathbf{r}' = (x', y', z')$ and $\mathbf{r} = (x, y, z)$ are position vectors corresponding to the source and the observation points, respectively. $\mathbf{k} = (k_x, k_y, k_z)$ is a wavenumber vector in free space, and $\mathbf{k}_{xy} = (k_x, k_y)$, $\boldsymbol{\rho}'_{xy} = (x', y')$, $\boldsymbol{\rho}_{xy} = (x, y)$. $\hat{\boldsymbol{\phi}}$ and $\hat{\boldsymbol{\theta}}$ are unit vectors corresponding to ϕ- and θ-directions in a spherical coordinate system, respectively. $\overline{\overline{\mathbf{G}}}^{\mathrm{D}}$ is a dyadic Green's function of free space and corresponds to direct wave from the source point to the observation point. $\overline{\overline{\mathbf{G}}}^{\mathrm{TE}}$ and $\overline{\overline{\mathbf{G}}}^{\mathrm{TM}}$ are dyadic Green's functions corresponding to the reflection waves from the 2-D infinite periodic array of scatterers. As mentioned earlier, effect of reflecting wave corresponding to evanescent wave on self/mutual coupling is neglected here. Therefore, it should be noted that. Equations (5)–(7) are reduced forms of the dyadic Green's functions. Formulation of (5)–(7) is described in Appendix.

C. Self/Mutual Impedance Expressions

According to the MoM based on an electric field integral equation, self/mutual impedance between the source and observation points over the 2-D infinite periodic array of scatters is expressed as follows:

$$\begin{aligned} Z_{ij} &= j\omega\mu_0 \iint_S \iint_{S'} \mathbf{f}_i(\mathbf{r}')\cdot\overline{\overline{\mathbf{G}}}(\mathbf{r},\mathbf{r}')\cdot\mathbf{f}_j(\mathbf{r})d\mathbf{r}'d\mathbf{r} \\ &= Z_{ij}^{\mathrm{D}} + Z_{ij}^{\mathrm{TE}} + Z_{ij}^{\mathrm{TM}} \\ Z_{ij}^{\mathrm{D}} &= j\omega\mu_0 \int_S\int_{S'} \mathbf{f}_i(\mathbf{r}')\cdot\overline{\overline{\mathbf{G}}}^{\mathrm{D}}(\mathbf{r},\mathbf{r}')\cdot\mathbf{f}_j(\mathbf{r})d\mathbf{r}'d\mathbf{r} \\ &= j\omega\mu_0 \int_S\int_{S'} \mathbf{f}_i(\mathbf{r}')\cdot\left(\overline{\overline{\mathbf{I}}} + \frac{\nabla\nabla}{k_0^2}\right) \\ &\quad \frac{e^{-jk_0|\mathbf{r}-\mathbf{r}'|}}{4\pi|\mathbf{r}-\mathbf{r}'|}\cdot\mathbf{f}_j(\mathbf{r})d\mathbf{r}'d\mathbf{r} \end{aligned} \tag{8}$$

$$\begin{aligned} &\approx \frac{\omega\mu_0 k_0}{8\pi^2}\int_0^{2\pi}\int_0^{\frac{\pi}{2}}\Bigg[\left\{\int_S e^{-j\mathbf{k}\cdot\mathbf{r}}\left(\mathbf{f}_j(\mathbf{r})\cdot\hat{\boldsymbol{\phi}}\right)d\mathbf{r}\right\} \\ &\quad \left\{\int_{S'} e^{j\mathbf{k}\cdot\mathbf{r}'}\left(\mathbf{f}_i(\mathbf{r}')\cdot\hat{\boldsymbol{\phi}}\right)d\mathbf{r}'\right\} + \left\{\int_S e^{-j\mathbf{k}\cdot\mathbf{r}}\left(\mathbf{f}_j(\mathbf{r})\cdot\hat{\boldsymbol{\theta}}\right)d\mathbf{r}\right\} \\ &\quad \left\{\int_{S'} e^{j\mathbf{k}\cdot\mathbf{r}'}\left(\mathbf{f}_i(\mathbf{r}')\cdot\hat{\boldsymbol{\theta}}\right)d\mathbf{r}'\right\}\Bigg]\sin\theta d\theta d\phi \end{aligned} \tag{9}$$

$$\begin{aligned} Z_{ij}^{\mathrm{TE}} &= j\omega\mu_0 \int_S\int_{S'} \mathbf{f}_i(\mathbf{r}')\cdot\overline{\overline{\mathbf{G}}}^{\mathrm{TE}}(\mathbf{r},\mathbf{r}')\cdot\mathbf{f}_j(\mathbf{r})d\mathbf{r}'d\mathbf{r} \\ &\approx \frac{\omega\mu_0 k_0}{8\pi^2}\int_0^{2\pi}\int_0^{\frac{\pi}{2}}\left\{\int_S e^{-j\left(\mathbf{k}_{xy}\cdot\boldsymbol{\rho}_{xy}+k_z z\right)}\left(\mathbf{f}_j(\mathbf{r})\cdot\hat{\boldsymbol{\phi}}\right)d\mathbf{r}\right\} \\ &\quad \Gamma_{z=d}^{\mathrm{TE}}(\theta,\phi)\left\{\int_{S'} e^{j\left(\mathbf{k}_{xy}\cdot\boldsymbol{\rho}'_{xy}-k'_z z\right)}\left(\mathbf{f}_i(\mathbf{r}')\cdot\hat{\boldsymbol{\phi}}\right)d\mathbf{r}'\right\} \\ &\quad \sin\theta d\theta d\phi \end{aligned} \tag{10}$$

$$\begin{aligned} Z_{ij}^{\mathrm{TM}} &= \frac{j\omega\mu_0}{k_0^2} \int_S\int_{S'} \mathbf{f}_i(\mathbf{r}')\cdot\overline{\overline{\mathbf{G}}}^{\mathrm{TM}}(\mathbf{r},\mathbf{r}')\cdot\mathbf{f}_j(\mathbf{r})d\mathbf{r}'d\mathbf{r} \\ &\approx \frac{\omega\mu_0 k_0}{8\pi^2}\int_0^{2\pi}\int_0^{\frac{\pi}{2}}\left\{\int_S e^{-j\left(\mathbf{k}_{xy}\cdot\boldsymbol{\rho}_{xy}+k_z z\right)}\left(\mathbf{f}_j(\mathbf{r})\cdot\hat{\boldsymbol{\theta}}\right)d\mathbf{r}\right\} \\ &\quad \Gamma_{z=d}^{\mathrm{TM}}(\theta,\phi)\left\{\int_{S'} e^{j\left(\mathbf{k}_{xy}\cdot\boldsymbol{\rho}'_{xy}-k'_z z\right)}\left(\mathbf{f}_i(\mathbf{r}')\cdot\hat{\boldsymbol{\theta}}\right)d\mathbf{r}'\right\} \\ &\quad \sin\theta d\theta d\phi. \end{aligned} \tag{11}$$

Here, $\mathbf{f}_i(\mathbf{r}')$ and $\mathbf{f}_j(\mathbf{r})$ are a basis function for current at the ith source point and a testing function for current at the jth observation point, respectively. S' and S are area where $\mathbf{f}_i(\mathbf{r}')$ and $\mathbf{f}_j(\mathbf{r})$ are defined. It is found that spatial integration over S' and S are completely separated for (9)–(11) because the reduced forms of the dyadic Green's function are expressed using a plane wave expansion. It should be noted that the mutual impedance corresponding to direct wave is obtained using (8), not (9) in practice. Equation (9) is used only for validating accuracy and convergence of the mutual impedance expressions using plane wave expansion as follows.

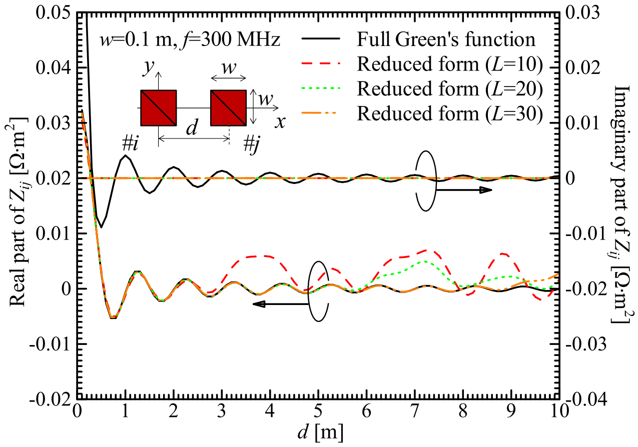

Fig. 2. Convergence of mutual impedance between two coplanar PEC plates obtained using reduced forms of dyadic Green's functions ($w = 0.1$ m).

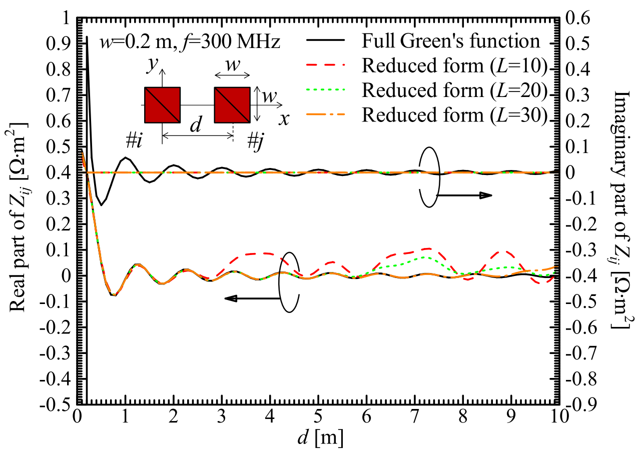

Fig. 3. Convergence of mutual impedance between two coplanar PEC plates obtained using reduced forms of dyadic Green's functions ($w = 0.2$ m).

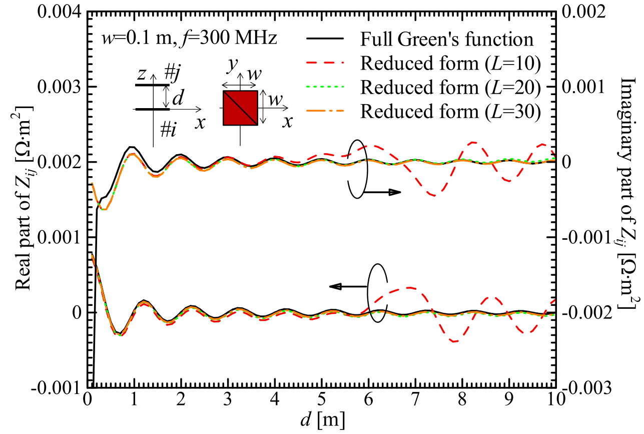

Fig. 4. Convergence of mutual impedance between two parallel PEC plates obtained using reduced forms of dyadic Green's functions ($w = 0.1$ m).

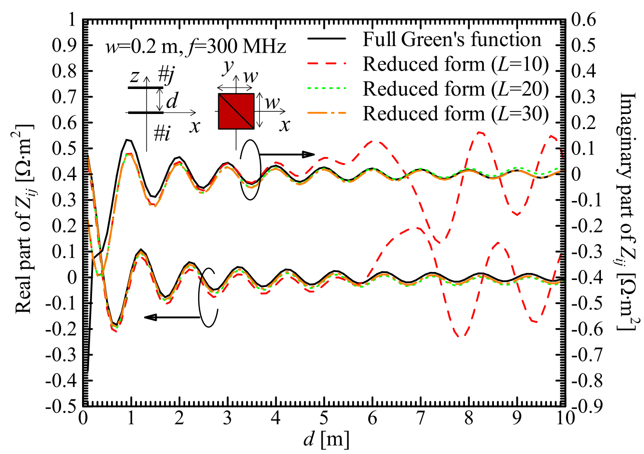

Fig. 5. Convergence of mutual impedance between two parallel PEC plates obtained using reduced forms of dyadic Green's functions ($w = 0.2$ m).

III. Numerical Simulation

A. Validation

Here, accuracy and convergence of the self/mutual impedance expressions using the reduced forms of the dyadic Green's functions are discussed in advance of numerical analysis of antennas over the 2-D infinite periodic array of scatterers. Figs. 2–5 show mutual impedance between two coplanar/parallel PEC plates. Mutual impedance between the plates is obtained using (8) and (9), i.e., the plates are in free space. Rao–Wilton–Glisson (RWG) basis function is used for both of the basis/testing functions [34]. Spatial integrals over S and S' of (9) are performed analytically whereas spectral integrals over θ and ϕ of (9) are performed numerically. Gauss–Legendre quadrature with L quadrature points and trapezoidal quadrature with $2L$ quadrature points are applied to numerical quadrature for θ and ϕ, respectively.

According to Figs. 2–5, it is found that a large number of quadrature points are necessary for convergence of mutual impedance obtained using (9) as spacing between the plates increases. As mentioned earlier, the reduced forms of the dyadic Green's functions are expressed by the plane wave expansion and complex exponential functions included in the reduced forms (i.e., $e^{-j\mathbf{k}\cdot\mathbf{r}}$ or $e^{j\mathbf{k}\cdot\mathbf{r}'}$) are highly oscillatory when $\mathbf{r}$ or $\mathbf{r}'$ increases. Therefore, convergence of the mutual impedance obtained using (9) is slow and a large number of quadrature points are necessary when the spacing between the plates increases. From a physical viewpoint, mutual coupling via far-field components is kept in (9) whereas that via evanescent wave components is lost. As a result, real part of the mutual impedance obtained using (9) agrees well with that obtained using (8) whereas relatively large discrepancy is found between its imagenary part and that using (8).

Fig. 6 shows input impedance of a planar dipole antenna on an infinite ground plane using the proposed method. In the proposed method, mutual coupling between the source and observation points via the infinite ground plane is obtained from (10) and (11) with $\Gamma^{\mathrm{TE}}_{z=0}(\theta,\phi) = -1$ for TE wave and $\Gamma^{\mathrm{TM}}_{z=0}(\theta,\phi) = 1$ for TM wave [28]. To clarify the performance of the proposed method, numerical results obtained using the MoM with the layered media Green's function (Full-wave) are shown [29], [30], [35]. Although the proposed method neglects the effect of the evanescent wave components, it is found that the numerical results obtained using both of the methods agree well each other.

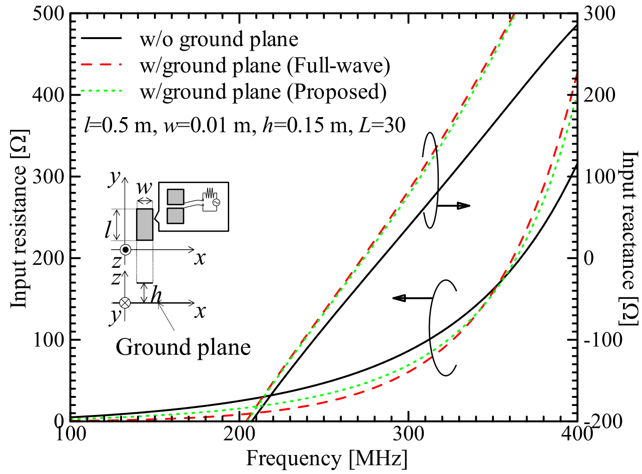

Fig. 6. Input impedance of planar dipole antenna on infinite ground plane.

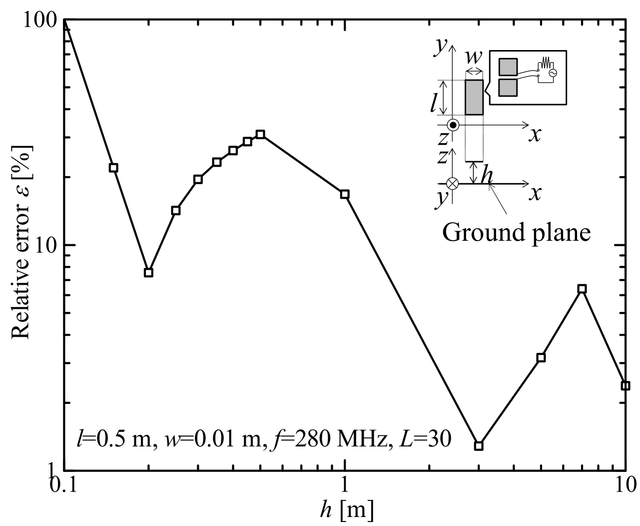

Fig. 7. Relative error of input impedance at resonant frequency of dipole antenna.

Accuracy and applicability of the proposed method are evaluated via a relative error of the input impedance which is defined as follows:

$$\varepsilon = \frac{|Z_{in}^{L}(f) - Z_{in}^{R}(f)|}{|Z_{in}^{L}(f)|}$$

where $Z_{in}^{L}(f)$ and $Z_{in}^{R}(f)$ are the input impedances at frequency f obtained using the layered media Green's function and its reduced forms, respectively. Fig. 7 shows a relative error of the input impedance of the planar dipole antenna on the infinite ground plane using the proposed method. It is found that the relative error is below 30% when $h > 0.15$ m (i.e., $\approx 0.14\lambda @ f = 280$ MHz). For example, the relative error is 22% for the input impedance at $f = 280$ MHz when $h = 0.15$ m. According to the results, it is expected that the proposed method works for numerical analysis of antennas over the 2-D infinite periodic array of the scatterers when $h > 0.14\lambda$. On the other hand, it is found that the proposed method suffers from large error when $h < 0.14\lambda$ because the effect of the evanescent wave which is neglected in the proposed method is dominant.

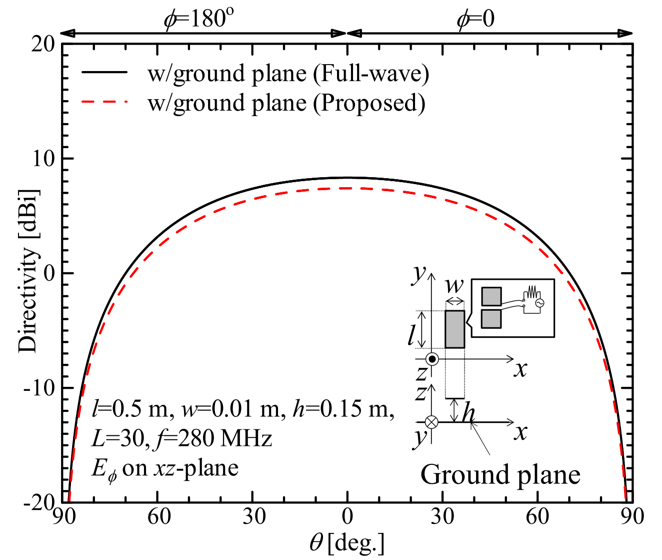

Fig. 8. Directivity of planar dipole antenna on infinite ground plane (E_ϕ on xz plane).

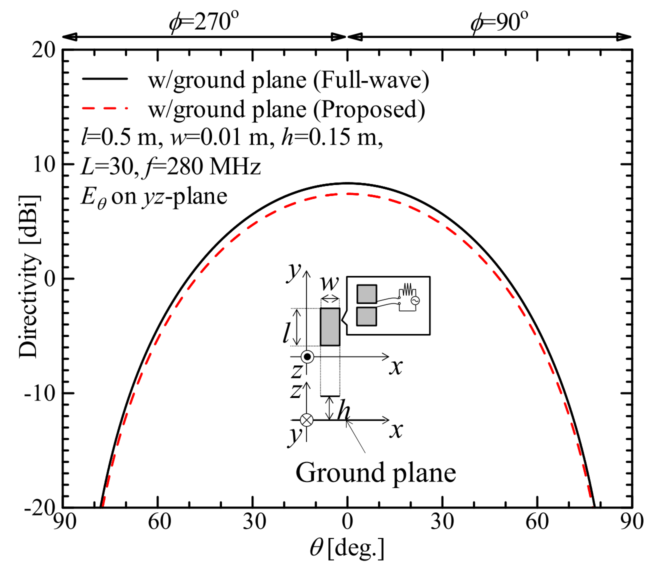

Fig. 9. Directivity of planar dipole antenna on infinite ground plane (E_θ on yz plane).

Directivities of the planar dipole antenna over the infinite ground plane are shown in Figs. 8 and 9. It is found that directivities obtained using the proposed method agree well with those of the full-wave analysis except fot small shift ($\approx$ 0.9 dB) of their magnitude.

B. Numerical Analysis of Antennas Over FSS

Here, antennas over a 2-D infinite periodic array of scatterers are numerically analyzed using the MoM with the reduced forms of the dyadic Green's functions. A planar dipole antenna over a planar dipole FSS and a rectangular loop antenna over a circular loop FSS are shown in Figs. 10 and 11, respectively. The antennas over the FSS are practically used for RCS reduction or multiband applications [36], [37], [38], and [39]. Although the antennas over the FSS in this work

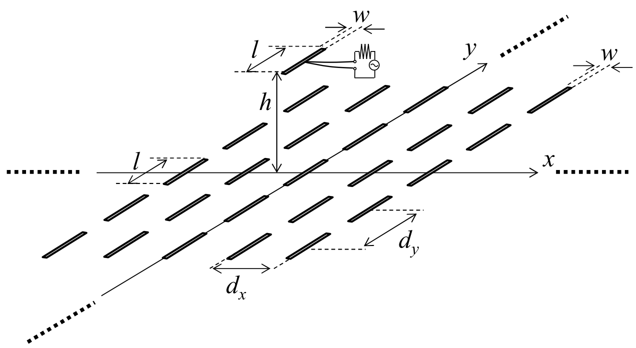

Fig. 10. Planar dipole antenna over planar dipole FSS.

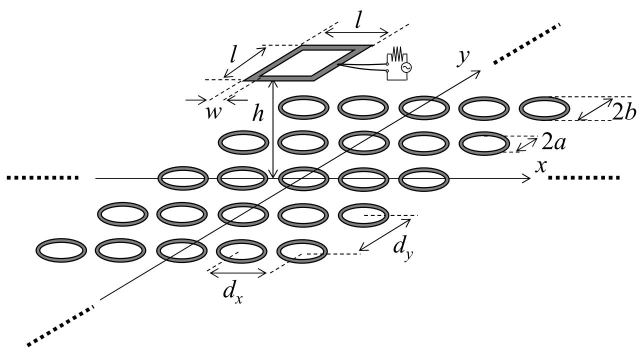

Fig. 11. Rectangular loop antenna over circular loop FSS.

have not been designed for specific applications, effect of the FSS on the radiation performance of the antennas can be demonstrated. In advance of numerical analysis of the antennas over the FSSs, reflection coefficients of the FSSs are calculated and tabulated. Our in-house code based on the MoM with the periodic Green's function is used for numerical analysis of the FSSs. Detailed descriptions on the periodic Green's function or relevant theories such as Floquet theorem are found in [2], [4], and [5]. Singularity at a source point is annihilated using L'Hospital rule [6], [7]. Poor convergence of the periodic Green's function is enhanced using Ewald transformation with the optimum splitting parameter [31], [32], and [33]. RWG basis function is used for both of the basis/testing functions [34].

Input impedance of the antennas over the FSSs is shown in Figs. 12 and 13. In the proposed method, (8) is used for calculating the self/mutual impedance corresponding to the direct wave whereas (10) and (11) are used for calculating those corresponding to the TE/TM reflection waves. Singularity where the source point and the observation point are overlapped is annihilated using coordinate transformation and analytic integral [40], [41]. Input impedance of both of the antennas over finite 7 × 7 FSSs and isolated antennas (w/o FSS) is also shown in Figs. 12 and 13 as references because full-wave analysis of the antennas over the infinite FSSs is unavailable. In advance of numerical analysis, it has been confirmed that the input impedance of the antennas over the finite FSSs converges even when the number of scatterers increase. According to Figs. 12 and 13, it is found that the effect of mutual coupling between the antenna and

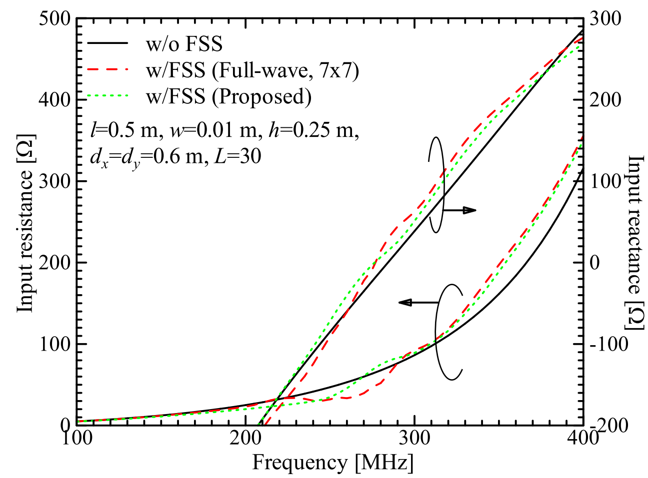

Fig. 12. Input impedance of planar dipole antenna over planar dipole FSS.

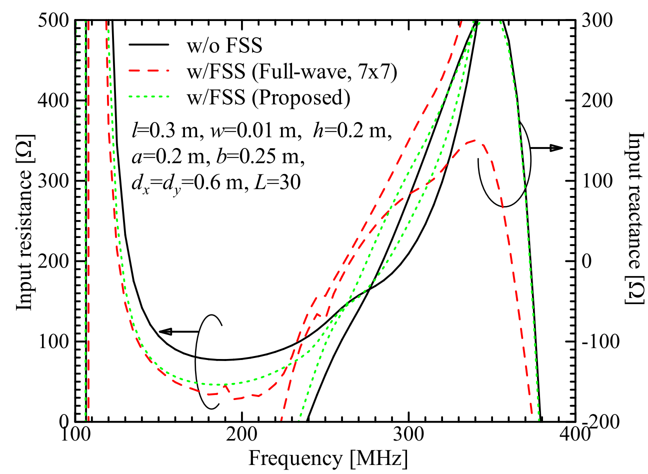

Fig. 13. Input impedance of rectangular loop antenna over circular loop FSS.

the scatterers is reflected to the input impedance obtained using the MoM with the reduced form of Green's function. As a result, the input impedance of the antennas over the infinite FSSs approaches to that over the finite 7 × 7 FSSs. Of course, perfect agreement between the input impedance of the planar dipole antennas over the infinite/finite FSSs is unavailable and a certain amount of discrepancy is found. The discrepancy between the input impedances stems from the effect of the evanescent wave that is lost from the reduced forms of the dyadic Green's functions. Therefore, it is expected that the discrepancy between the input impedances become small as h increases as shown in Fig. 7.

Directivities of the antennas over the FSSs in xz plane are shown in Figs. 14 and 15. It is found that the directivity of the planar dipole antenna over the planar dipole FSS drops around $\theta = 40°$. whereas that of the rectangular loop antenna over the circular loop FSS is roughly omnidirectional. To clarify the effect of the FSSs on the directivities of the antennas, reflection coefficients of the FSSs are shown in Figs. 16 and 17. As shown in Fig. 16, the planar dipole FSS is transparent around $\theta = 40°$. whereas it is opaque at remaining angles. Therefore, it is found that the drop of the

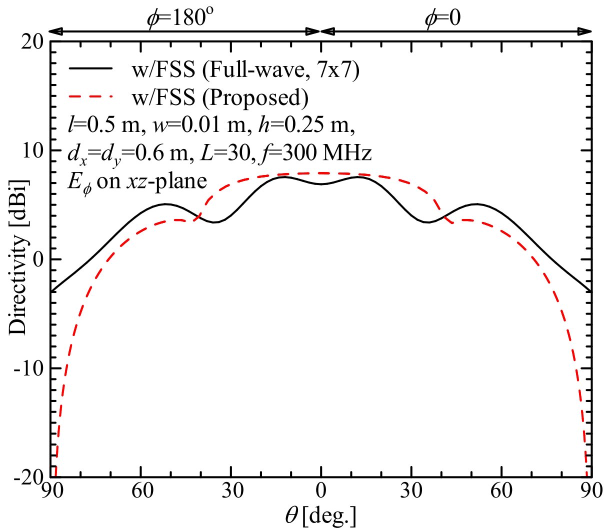

Fig. 14. Directivity of planar dipole antenna over planar dipole FSS (E_ϕ on xz plane).

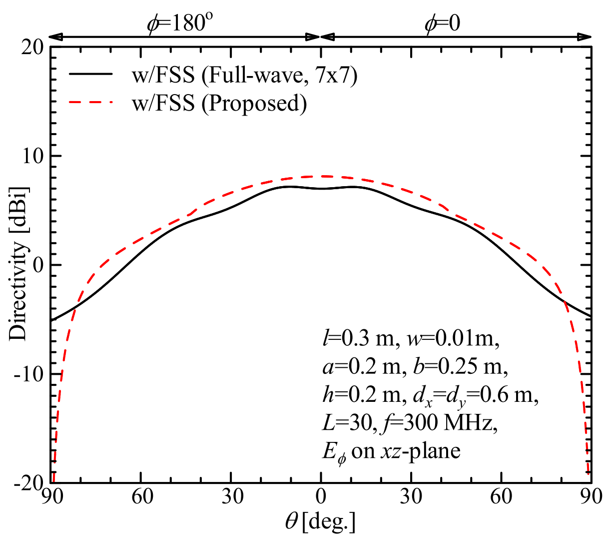

Fig. 15. Directivity of rectangular loop antenna over circular loop FSS (E_ϕ on xz plane).

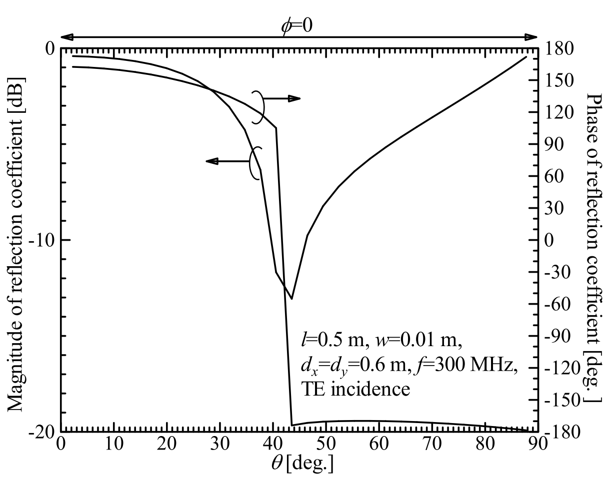

Fig. 16. Reflection coefficient of planar dipole FSS [TE incidence on xz plane, $\Gamma^{\mathrm{TE}}_{z=0}(\theta, \phi = 0)$].

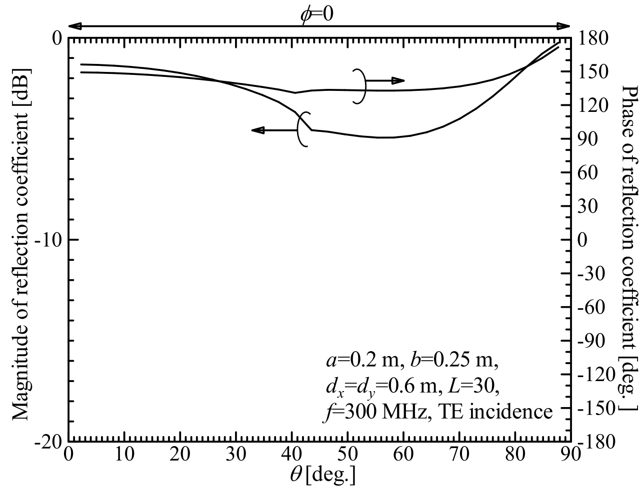

Fig. 17. Reflection coefficient of circular loop FSS [TE incidence on xz plane, $\Gamma^{\mathrm{TE}}_{z=0}(\theta, \phi = 0)$].

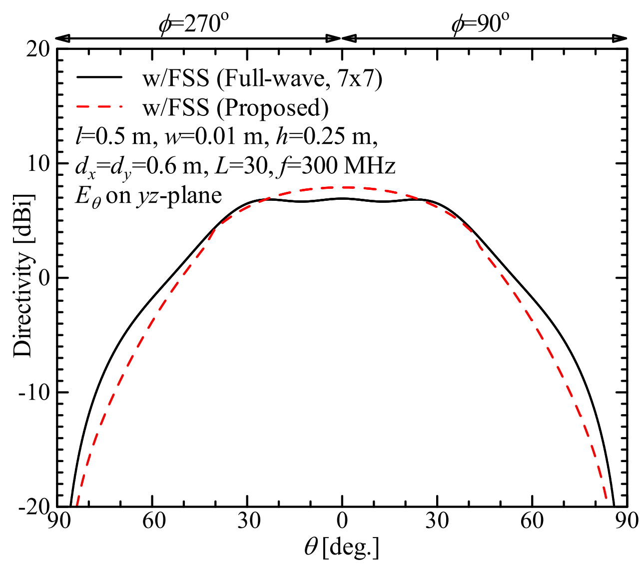

Fig. 18. Directivity of planar dipole antenna over planar dipole FSS (E_θ on yz plane).

directivity around $\theta = 40°$. comes from reflection performance of the planar dipole FSS. On the other hand, the circular loop FSS is roughly opaque over all angles of θ as shown in Fig. 17. Therefore, it can be said that reflection performance of the circular loop FSS is similar to that of the ground plane in xz plane. As a result, directivity of the rectangular loop antenna over the circular loop FSS is similar to that of the planar dipole antenna over the ground plane as shown in Fig. 8. Although perfect agreement between directivities of the antennas over infinite/finite FSSs is unavailable, their main lobe levels and radiation patterns are found to be comparable. Ideally, directivities obtained using the proposed MoM are expected to agree with those using the full-wave MoM if the full-wave MoM can deal with the antennas over the infinite FSSs. Directivities of the antennas over the FSSs in yz plane shown in Figs. 18 and 19 can also be explained by the reflection coefficients of the FSSs shown in Figs. 20 and 21. The discussion is lengthy and omitted here.

Computational cost of the MoM with the reduced form of Green's function is tabulated in Table I. Here, the total

TABLE I
COMPUTATIONAL COST

	Planar dipole over planar dipole FSS		Rectangular loop over circular loop FSS	
Size of FSS	Finite, 7×7	Infinite	Finite, 7×7	Infinite
Analysis method	Full-wave	Proposed ($L = 30$)	Full-wave	Proposed ($L = 30$)
Number of frequency points	61			
Number of unknowns N	750	15	2249	44
Total CPU time for matrix filling [sec.]	93	28	683	205
Total CPU time for matrix inversion [sec.]	1041	Negligible	23784	Negligible

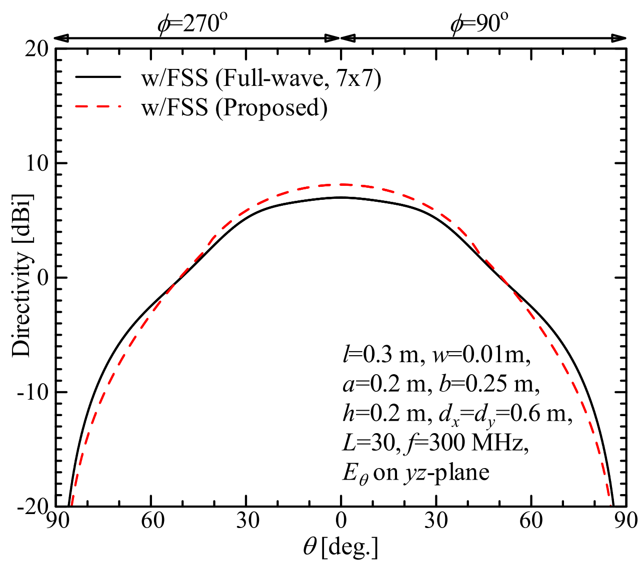

Fig. 19. Directivity of rectangular loop antenna over circular loop FSS (E_θ on yz plane).

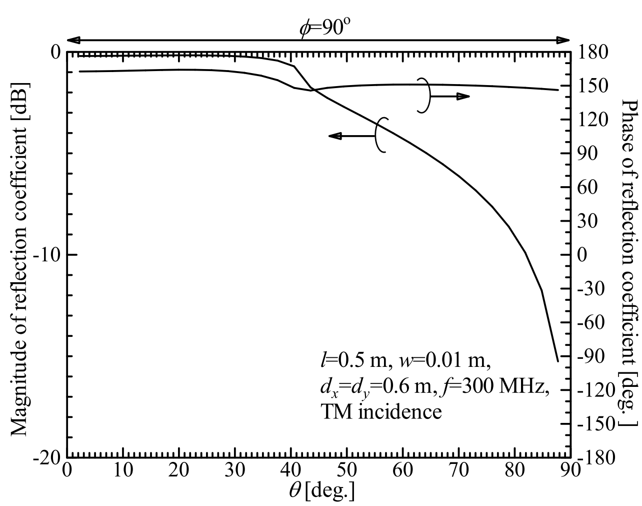

Fig. 20. Reflection coefficient of planar dipole FSS [TM incidence on yz plane, $\Gamma^{\mathrm{TM}}_{z=0}(\theta, \phi = 90°)$].

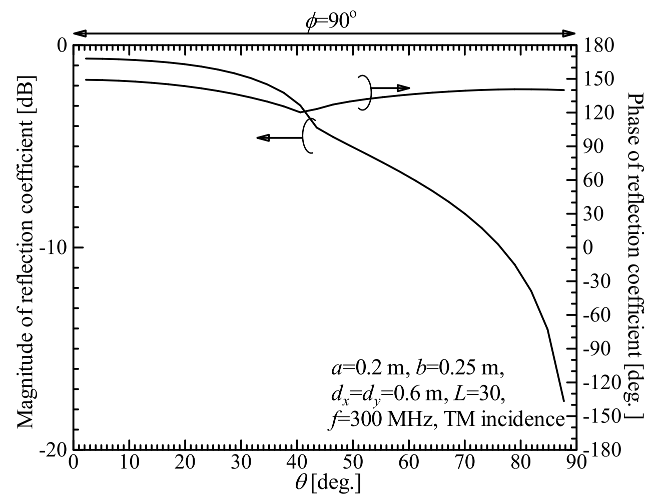

Fig. 21. Reflection coefficient of circular loop FSS [TM incidence on yz plane, $\Gamma^{\mathrm{TM}}_{z=0}(\theta, \phi = 90°)$].

CPU time for numerical analysis of the antennas over the FSS at 61 frequency points from 100 to 400 MHz is tabulated. According to Table I, it is found that the total CPU time for numerical analysis of the antennas over the finite FSS is long because of the large number of unknowns N. On the other hand, the total CPU time for numerical analysis of the antennas over the infinite FSS using the MoM with the reduced forms of the dyadic Green's function is short because of the small number of unknowns N. Therefore, it can be concluded that the MoM with the reduced form of Green's function is an efficient technique for numerical analysis of the antennas over the 2-D infinite periodic array of scatterers.

IV. Conclusion

In this article, a novel MoM for numerical analysis of antennas over a 2-D infinite periodic array of scatterers has been proposed. The proposed MoM models the 2-D infinite periodic array of scatterers as a reflecting plane and its electromagnetic response is formulated as a Green's function. Electromagnetic waves from the source point to the observation point over the 2-D in finite periodic array of scatterers are expressed as summation of a direct wave and TE/TM reflection waves. The direct wave is expressed using the free space Green's function whereas the TE/TM reflection waves is expressed using the numerically obtained reflection coefficients with the plane wave expansion. Because the electromagnetic response of the two-dimensional infinite periodic array of scatterers is expressed via reflection coefficients, the proposed MoM is mesh-free for the 2-D infinite periodic array of scatterers. Numerical simulation was performed, and it has been demonstrated that the proposed MoM works efficiently for numerical analysis of the arbitrary-shaped antennas over the 2-D infinite periodic array of the arbitrary-shaped scatterers.

Although performance of the proposed MoM has been demonstrated in this article, a couple of problems to be challenged are still remaining. The first one is modeling of the effect of the evanescent waves. The evanescent waves from the 2-D infinite periodic array of scatterers correspond to higher order Floquet modes that are absent in this work. Modeling of the effect of the evanescent waves is not easy because the reflection coefficients of the 2-D infinite periodic array of scatterers corresponding to the higher order Floquet modes could be tensor, not scalar, i.e., TM components of reflection waves come from TE incidence and vice versa. The second one is efficient computation of the reflection coefficients of the 2-D infinite periodic array of scatterers. As mentioned earlier, a large number of quadrature points L are necessary for calculating mutual impedance between source and observation points as their spacing increase. Therefore, an efficient computation method of the reflection coefficients is necessary for numerical analysis of large-scale antennas over the 2-D infinite periodic array of scatterers. These problems are challenges in the future.

Appendix
Formulation of Reduced Form of Dyadic Green's Function

Here, the reduced form of the dyadic Green's function in a space above the 2-D infinite periodic array of scatterers is derived starting from the layered media Green's function. For convenience, the layered media Green's function is revisited as follows:

$$\overline{\overline{\mathbf{G}}}(\mathbf{r},\mathbf{r}') = \overline{\overline{\mathbf{G}}}^{\mathrm{D}}(\mathbf{r},\mathbf{r}') + \overline{\overline{\mathbf{G}}}^{\mathrm{TE}}(\mathbf{r},\mathbf{r}') + \frac{1}{k_0^2}\overline{\overline{\mathbf{G}}}^{\mathrm{TM}}(\mathbf{r},\mathbf{r}')$$

$$\overline{\overline{\mathbf{G}}}^{\mathrm{D}}(\mathbf{r},\mathbf{r}') = \left(\overline{\overline{\mathbf{I}}} + \frac{\nabla\nabla}{k_0^2}\right)\frac{e^{-jk_0|\mathbf{r}-\mathbf{r}'|}}{4\pi|\mathbf{r}-\mathbf{r}'|} \tag{12}$$

$$\overline{\overline{\mathbf{G}}}^{\mathrm{TE}}(\mathbf{r},\mathbf{r}') = (\nabla\times\hat{z})(\nabla'\times\hat{z})g^{\mathrm{TE}}(\mathbf{r},\mathbf{r}') \tag{13}$$

$$\overline{\overline{\mathbf{G}}}^{\mathrm{TM}}(\mathbf{r},\mathbf{r}') = (\nabla\times\nabla\times\hat{z})(\nabla'\times\nabla'\times\hat{z})g^{\mathrm{TM}}(\mathbf{r},\mathbf{r}') \tag{14}$$

$$g^{\mathrm{TE}}(\mathbf{r},\mathbf{r}') = -\frac{j}{8\pi^2}\int_{-\infty}^{\infty}\int_{-\infty}^{\infty}\frac{e^{j\mathbf{k}_{xy}\cdot(\boldsymbol{\rho}_{xy}-\boldsymbol{\rho}'_{xy})}F^{\mathrm{TE}}}{k_z(k_x^2+k_y^2)}dk_x dk_y \tag{15}$$

$$g^{\mathrm{TM}}(\mathbf{r},\mathbf{r}') = -\frac{j}{8\pi^2}\int_{-\infty}^{\infty}\int_{-\infty}^{\infty}\frac{e^{j\mathbf{k}_{xy}\cdot(\boldsymbol{\rho}_{xy}-\boldsymbol{\rho}'_{xy})}F^{\mathrm{TM}}}{k_z(k_x^2+k_y^2)}dk_x dk_y. \tag{16}$$

According to well-known Weyl identity, a scalar Green's function in free space shown in (12) is expressed in spectral domain as follows:

$$\frac{e^{-jk_0|\mathbf{r}-\mathbf{r}'|}}{|\mathbf{r}-\mathbf{r}'|} = \frac{-j}{2\pi}\int_{-\infty}^{\infty}\int_{-\infty}^{\infty}\frac{e^{-j\{\mathbf{k}_{xy}\cdot(\boldsymbol{\rho}_{xy}-\boldsymbol{\rho}'_{xy})+k_z|z-z'|\}}}{k_z}dk_x dk_y. \tag{17}$$

According to reciprocity, it is assumed that $z-z' \geq 0$ without loss of generality. Therefore, (17) can be reduced under the assumption of $k_z^2 = k_0^2 - k_x^2 - k_y^2 \geq 0$ as follows:

$$\begin{aligned}\frac{e^{-jk_0|\mathbf{r}-\mathbf{r}'|}}{|\mathbf{r}-\mathbf{r}'|} &\approx \frac{-j}{2\pi}\iint_{k_x^2+k_y^2\leq k_0^2}\frac{e^{-j\mathbf{k}\cdot(\mathbf{r}-\mathbf{r}')}}{k_z}dk_x dk_y \\ &= \frac{-j}{2\pi}\int_0^{k_0}\int_0^{2\pi}\frac{e^{-j\mathbf{k}\cdot(\mathbf{r}-\mathbf{r}')}}{\sqrt{k_0-\xi^2}}\xi d\phi d\xi \\ &\qquad (\because k_x \equiv \xi\cos\phi,\ k_y \equiv \xi\sin\phi) \\ &= \frac{-jk_0}{2\pi}\int_0^{\frac{\pi}{2}}\int_0^{2\pi}e^{-j\mathbf{k}\cdot(\mathbf{r}-\mathbf{r}')}\sin\theta d\phi d\theta \\ &\qquad (\because \xi \equiv k_0\sin\theta).\end{aligned} \tag{18}$$

Once (18) is substituted into (12), (5) is readily obtained. In the same manner as deriving (18), (6) and (7) are obtained from (13) to (16). The equivalent expression of (18) is found in previous works [42], [43].

Acknowledgment

Discussions with the members of the Cooperative Research Project Program of the Research Institute of Electrical Communication, Tohoku University, Sendai, Japan, were helpful for this work.

References

[1] L. Stark, "Radiation impedance of a dipole in an infinite planar phased array," *Radio Sci.*, vol. 1, no. 3, pp. 361–377, Mar. 1966.

[2] B. A. Munk, *Frequency Selective Surfaces: Theory and Design*. New York, NY, USA: Wiley, 2000.

[3] J. Huang and J. A. Encinar, *Reflectarray Antennas*. Hoboken, NJ, USA: Wiley, 2008.

[4] M. G. Floquet, "Sur les équations différentielles linéaires à coefficients périodiques," in *Annales Scientifiques de L'École Normale Supérieure*. France: Gauthier-Villars, 1883, pp. 47–88.

[5] T. F. Eibert, J. L. Volakis, D. R. Wilton, and D. R. Jackson, "Hybrid FE/BI modeling of 3-D doubly periodic structures utilizing triangular prismatic elements and an MPIE formulation accelerated by the Ewald transformation," *IEEE Trans. Antennas Propag.*, vol. 47, no. 5, pp. 843–850, May 1999.

[6] I. Stevanoviæ and J. R. Mosig, "Periodic Green's function for skewed 3-D lattices using the Ewald transformation," *Microw. Opt. Technol. Lett.*, vol. 49, no. 6, pp. 1353–1357, Jun. 2007.

[7] J. Su, X.-W. Xu, M. He, and K. Zhang, "Integral-equation analysis of frequency selective surfaces using Ewald transformation and lattice symmetry," *Prog. Electromagn. Res.*, vol. 121, pp. 249–269, 2011.

[8] D. Sievenpiper, L. Zhang, R. F. J. Broas, N. G. Alexopolous, and E. Yablonovitch, "High-impedance electromagnetic surfaces with a forbidden frequency band," *IEEE Trans. Microw. Theory Techn.*, vol. 47, no. 11, pp. 2059–2074, Nov. 1999.

[9] K. M. Shum, Q. Xue, C. H. Chan, and K. M. Luk, "Investigation of microstrip reflectarray using a photonic bandgap structure," *Microw. Opt. Technol. Lett.*, vol. 28, no. 2, pp. 114–116, Jan. 2001.

[10] V. V. S. Prakash and R. Mittra, "Characteristic basis function method: A new technique for efficient solution of method of moments matrix equations," *Microw. Opt. Technol. Lett.*, vol. 36, no. 2, pp. 95–100, Jan. 2003.

[11] D. J. Ludick, M. M. Botha, R. Maaskant, and D. B. Davidson, "The CBFM-enhanced Jacobi method for efficient finite antenna array analysis," *IEEE Antennas Wireless Propag. Lett.*, vol. 16, pp. 2700–2703, 2017.

[12] K. Konno, Q. Chen, and R. J. Burkholder, "Numerical analysis of large-scale finite periodic arrays using a macro block-characteristic basis function method," *IEEE Trans. Antennas Propag.*, vol. 65, no. 10, pp. 5348–5355, Oct. 2017.

[13] Y. Zhuang, K.-L. Wu, C. Wu, and J. Litva, "A combined full-wave CG-FFT method for rigorous analysis of large microstrip antenna arrays," *IEEE Trans. Antennas Propag.*, vol. 44, no. 1, pp. 102–109, Jan. 1996.

[14] P. Janpugdee, P. H. Pathak, P. Mahachoklertwattana, and R. J. Burkholder, "An accelerated DFT-MoM for the analysis of large finite periodic antenna arrays," *IEEE Trans. Antennas Propag.*, vol. 54, no. 1, pp. 279–283, Jan. 2006.

[15] H. Zhai, Q. Yuan, Q. Chen, and K. Sawaya, "Preconditioners for CG-FMM-FFT implementation in EM analysis of large-scale periodic array antennas," *IEICE Trans. Commun.*, vol. 90, no. 3, pp. 707–710, Mar. 2007.

[16] R. Sigelmann and A. Ishimaru, "Radiation from periodic structures excited by an aperiodic source," *IEEE Trans. Antennas Propag.*, vol. AP-13, no. 3, pp. 354–364, May 1965.

[17] C. P. Wu and V. Galindo, "Properties of a phased array of rectangular waveguides with thin walls," *IEEE Trans. Antennas Propag.*, vol. AP-14, no. 3, pp. 163–173, Mar. 1966.

[18] B. A. Munk and G. A. Burrell, "Plane-wave expansion for arrays of arbitrarily oriented piecewise linear elements and its application in determining the impedance of a single linear antenna in a lossy half-space," *IEEE Trans. Antennas Propag.*, vol. AP-27, no. 5, pp. 331–343, May 1979.

[19] H.-Y. D. Yang and D. R. Jackson, "Theory of line-source radiation from a metal-strip grating dielectric-slab structure," *IEEE Trans. Antennas Propag.*, vol. 48, no. 4, pp. 556–564, Apr. 2000.

[20] F. Capolino, D. R. Jackson, and D. R. Wilton, "Fundamental properties of the field at the interface between air and a periodic artificial material excited by a line source," *IEEE Trans. Antennas Propag.*, vol. 53, no. 1, pp. 91–99, Jan. 2005.

[21] F. Capolino, D. R. Jackson, and D. R. Wilton, "Mode excitation from sources in two-dimensional EBG waveguides using the array scanning method," *IEEE Microw. Wireless Compon. Lett.*, vol. 15, no. 2, pp. 49–51, Feb. 2005.

[22] R. Qiang, J. Chen, F. Capolino, D. R. Jackson, and D. R. Wilton, "ASM–FDTD: A technique for calculating the field of a finite source in the presence of an infinite periodic artificial material," *IEEE Microw. Wireless Compon. Lett.*, vol. 17, no. 4, pp. 271–273, Apr. 2007.

[23] F. Capolino, D. R. Jackson, D. R. Wilton, and L. B. Felsen, "Comparison of methods for calculating the field excited by a dipole near a 2-D periodic material," *IEEE Trans. Antennas Propag.*, vol. 55, no. 6, pp. 1644–1655, Jun. 2007.

[24] F. Bilotti, L. Vegni, and F. Viviani, "Spectral dyadic Green's function of integrated structures with high impedance ground planes," *J. Electromagn. Waves Appl.*, vol. 17, no. 10, pp. 1461–1484, Jan. 2003.

[25] A. M. Attiya, "Dyadic Green's function of an elementary point source above a periodically-defected-grounded dielectric slab," *Prog. Electromagn. Res. B*, vol. 4, pp. 127–145, 2008.

[26] S. A. Tretyakov and C. R. Simovski, "Dynamic model of artificial reactive impedance surfaces," *J. Electromagn. Waves Appl.*, vol. 17, no. 1, pp. 131–145, Jan. 2003.

[27] T. Uno, T. Arima, and A. Kurahara, "FDTD modeling of nonperiodic antenna located above metasurface using surface impedance boundary condition," *EPJ Appl. Metamat.*, vol. 6, no. 17, pp. 1–7, Jul. 2019.

[28] W. C. Chew, *Waves and Fields in Inhomogenous Media*. New York, NY, USA: IEEE Press, 1995.

[29] W. C. Chew, J. L. Xiong, and M. A. Saville, "A matrix-friendly formulation of layered medium Green's function," *IEEE Antennas Wireless Propag. Lett.*, vol. 5, pp. 490–494, 2006.

[30] Y. P. Chen, W. C. Chew, and L. Jiang, "A new Green's function formulation for modeling homogeneous objects in layered medium," *IEEE Trans. Antennas Propag.*, vol. 60, no. 10, pp. 4766–4776, Oct. 2012.

[31] T. F. Eibert, J. L. Volakis, D. R. Wilton and D. R. Jackson, "Hybrid FE/BI modeling of 3-D doubly periodic structures utilizing triangular prismatic elements and an MPIE formulation accelerated by the Ewald transformation," *IEEE Trans. Antennas Propag.*, vol. 47, no. 5, pp. 843–850, May 1999, doi: 10.1109/8.774139.

[32] P. P. Ewald, "Die berechnung optischer und elektrostatischer gitterpotentiale," *Annalen Der Physik*, vol. 64, pp. 253–287, Mar. 1921.

[33] K. E. Jordan, G. R. Richter, and P. Sheng, "An efficient numerical evaluation of the Green's function for the Helmholtz operator on periodic structures," *J. Comp. Phys.*, vol. 63, pp. 222–235, Mar. 1986.

[34] S. Rao, D. Wilton, and A. Glisson, "Electromagnetic scattering by surfaces of arbitrary shape," *IEEE Trans. Antennas Propag.*, vol. AP-30, no. 3, pp. 409–418, May 1982.

[35] K. Konno, Q. Chen, and R. J. Burkholder, "Fast computation of layered media Green's function via recursive Taylor expansion," *IEEE Antennas Wireless Propag. Lett.*, vol. 16, pp. 1048–1051, 2017.

[36] S. Genovesi, F. Costa, and A. Monorchio, "Low-profile array with reduced radar cross section by using hybrid frequency selective surfaces," *IEEE Trans. Antennas Propag.*, vol. 60, no. 5, pp. 2327–2335, May 2012.

[37] Y. Chen, L. Chen, H. Wang, X.-T. Gu, and X.-W. Shi, "Dual-band crossed-dipole reflectarray with dual-band frequency selective surface," *IEEE Antennas Wireless Propag. Lett.*, vol. 12, pp. 1157–1160, 2013.

[38] M. Pazokian, N. Komjani, and M. Karimipour, "Broadband RCS reduction of microstrip antenna using coding frequency selective surface," *IEEE Antennas Wireless Propag. Lett.*, vol. 17, no. 8, pp. 1382–1385, Aug. 2018.

[39] W. Li, Y. Wang, S. Sun, and X. Shi, "An FSS-backed reflection/transmission reconfigurable array antenna," *IEEE Access*, vol. 8, pp. 23904–23911, 2020.

[40] R. D. Graglia, "On the numerical integration of the linear shape functions times the 3-D Green's function or its gradient on a plane triangle," *IEEE Trans. Antennas Propag.*, vol. 41, no. 10, pp. 1448–1455, Oct. 1993.

[41] D. Wilton, S. Rao, A. Glisson, D. Schaubert, O. Al-Bundak, and C. Butler, "Potential integrals for uniform and linear source distributions on polygonal and polyhedral domains," *IEEE Trans. Antennas Propag.*, vol. AP-32, no. 3, pp. 276–281, Mar. 1984.

[42] L. Greengard, J. Huang, V. Rokhlin, and S. Wandzura, "Accelerating fast multipole methods for the Helmholtz equation at low frequencies," *IEEE Comput. Sci. Eng.*, vol. 5, no. 3, pp. 32–38, 1998.

[43] M. Ayatollahi and S. Safavi-Naeini, "A fast analysis method based on exponential expansion of Green's function for large multilayer structures," in *Proc. IEEE Antennas Propag. Soc. Int. Symp.*, Jul. 2001, pp. 850–853.

Keisuke Konno (Member, IEEE) received the B.E., M.E., and D.E. degrees from Tohoku University, Sendai, Japan, in 2007, 2009, and 2012, respectively.

Since 2012, he has been with the Department of Communications Engineering, Graduate School of Engineering, Tohoku University, where he is currently an Associate Professor. He was with the ElectroScience Laboratory, The Ohio State University, Columbus, OH, USA, as a Visiting Scholar, from 2015 to 2017. His research interests include computational electromagnetics, array antennas, reflectarrays, and source reconstruction.

Dr. Konno is a member of the Institute of Electronics, Information and Communication Engineers (IEICE). He has received the JSPS Post-Doctoral Fellowships for Research Abroad. He has also received the Encouragement Award for Young Researcher and the Most Frequent Presentations Award in 2010 from the Technical Committee on Antennas and Propagation, Japan; the Young Researchers Award in 2011 from IEICE, Japan; the IEEE Electromagnetic Compatibility (EMC) Society Sendai Chapter Student Brush-Up Session and the EMC Sendai Seminar Student Best Presentation Award in 2011; the JSPS Washington Director Award in 2016; the MHz Rectenna Award in 2017; the Young Researchers Award for Group of Electrical Engineering, Communication Engineering, Electronic Engineering, and Information Engineering (ECEI) of Tohoku University in 2018; the Minoru Ishida Award in 2018; the IEEE AP-S Japan Young Engineer Award in 2018; the TOKIN Foundation Research Encouragement Award in 2019; and the IEICE Communications Society Distinguished Contributions Awards in 2019 and 2021.

Nozomi Haga (Member, IEEE) was born in Yamagata, Japan, in January 1985. He received the B.E., M.E., and D.E. degrees from Chiba University, Chiba, Japan, in 2007, 2009, and 2012, respectively.

Since 2012 to 2023, he has been an Assistant Professor at the Graduate School of Science and Technology, Gunma University, Gunma, Japan. Since 2023, he has been an Associate Professor at the Department of Electrical and Electronic Information Engineering, Toyohashi University of Technology, Toyohashi, Japan. His main research interests include electrically small antennas, body-centric wireless communication channels, and wireless power transfer systems.

Dr. Haga has received the Institute of Electronics, Information and Communication Engineers (IEICE) Technical Committee on Antennas and Propagation: Young Researcher Award in 2012, the IEICE Technical Committee on Wireless Power Transfer: Young Researcher Award in 2018, and the IEEE Antennas and Propagation Society Japan Young Engineer Award in 2018.

Jerdvisanop Chakarothai (Senior Member, IEEE) was born in Surat Thani, Thailand, in 1979. He received the B.E. degree in electrical and electronic engineering from Akita University, Akita, Japan, in 2003, and the M.S. and Ph.D. degrees in electrical and communication engineering from Tohoku University, Sendai, Japan, in 2005 and 2010, respectively.

He is currently a Senior Researcher with the National Institute of Information and Communications Technology, Koganei, Tokyo, Japan. His research interests include computational Electromagnetics (EM), biomedical communications, and electromagnetic compatibility (EMC).

Dr. Chakarothai is a member of the Institute of Electronics, Information and Communication Engineers (IEICE), the Institute of Electrical Engineers, Japan (IEEJ), and the Applied Computational Electromagnetic Society (ACES). He is an Expert Member of International Electrotechnical Commission (IEC) Comité International Spécial des Perturbations Radioélectriques (CISPR) Subcommittee A. He has received the 2014 Young Scientist Award from the International Scientific Radio Union and the Best Presentation Award from IEEJ and IEICE in 2015 and 2018, respectively. He has also received the Ulrich L. Rohde Innovative Conference Paper Award on antenna measurements and application in 2018, the Invited Paper Award from the Electronics Society of IEICE in 2020, and the Best Paper Award in International Symposium on Antennas and Propagations (ISAP) in 2021.

Qiang Chen (Senior Member, IEEE) received the B.E. degree from Xidian University, Xi'an, China, in 1986, and the M.E. and D.E. degrees from Tohoku University, Sendai, Japan, in 1991 and 1994, respectively.

He is currently the Chair Professor of the Electromagnetic Engineering Laboratory, Department of Communications Engineering, Faculty of Engineering, Tohoku University. His primary research interests include antennas, microwave and millimeter wave, electromagnetic measurement, and computational electromagnetics.

Dr. Chen is a fellow of the Institute of Electronics, Information and Communication Engineers (IEICE). He has received the Best Paper Award and the Zen-Ichi Kiyasu Award from IEICE. He has served as the Chair for the IEICE Technical Committee on Photonics-Applied Electromagnetic Measurement from 2012 to 2014, the IEICE Technical Committee on Wireless Power Transfer from 2016 to 2018, the IEEE Antennas and Propagation Society Tokyo Chapter from 2017 to 2018, and the IEICE Technical Committee on Antennas and Propagation from 2019 to 2021.

Narihiro Nakamoto (Member, IEEE) was born in Hyogo, Japan, in 1981. He received the B.E. and M.E. degrees in electrical engineering from Kyoto University, Kyoto, Japan, in 2005 and 2007, respectively.

In 2007, he joined Mitsubishi Electric Corporation, Kamakura, Kanagawa, Japan. From 2010 to 2012, he was with the Advanced Telecommunications Research Institute International (ATR) Wave Engineering Laboratories, Kyoto. In 2012, he returned to Mitsubishi Electric Corporation. Since then, he has been engaged in research and development of array antennas for satellite communication and radar systems.

Mr. Nakamoto is a Regular Member of the Institute of Electronics, Information and Communication Engineers (IEICE), Japan. He has received the IEEE Antennas and Propagation Society Tokyo Chapter Young Engineer Award in 2013 and the Young Engineer Award of IEICE in 2012.

Toru Takahashi (Senior Member, IEEE) was born in Kanagawa, Japan, in January 1970. He received the B.E. and M.E. degrees in electrical engineering and the D.E. degree from Waseda University, Tokyo, Japan, in 1992, 1994, and 2010, respectively.

In 1994, he joined Mitsubishi Electric Corporation, Kamakura, Japan, where he has been engaged in research and development on antennas, radar systems, and radio communication systems. He is currently the Manager of the Antennas Technology Department, Information Technology Research and Development Center.

Dr. Takahashi is a Senior Member of the Institute of Electronics, Information and Communication Engineers (IEICE), Japan. He has received the Young Engineer Award from IEICE in 1999 and the IEICE Communications Society Best Paper Award in 2013 and 2018.